

A Statistical Model to Predict the Strength Development of Geopolymer Concrete Based on $\text{SiO}_2/\text{Al}_2\text{O}_3$ Ratio Variation

Ali A. Ali ¹, Tareq S. Al-Attar ¹ , Waleed A. Abbas ^{1*} 

¹ Civil Engineering Department, University of Technology, Baghdad, Iraq.

Received 12 November 2021; Revised 26 January 2022; Accepted 09 February 2022; Published 01 March 2022

Abstract

Geopolymer Concrete (GPC) is a new class of concrete that presents a vital improvement in sustainability and the environment, particularly in recycling and alternative construction methods. Geopolymers offer a sustainable, low energy consumption, low carbon footprint, and a 100% substitute for the Portland cement binder for civil infrastructure applications. Furthermore, many aluminosilicate materials can be obtained as by-products of other processes, such as coal combustion or the thermal pulping of wood. In addition, slag and fly ash are necessary to source materials for geopolymer. Therefore, geopolymer is considered a solution for waste management that can minimize greenhouse gas emissions. In this statistical study, the present experimental work and found experimental data were collected from local and international literature and were used to build and validate the statistical models to predict the strength development of Geopolymer concrete with binary and ternary systems of source materials. The main independent variable was R, representing the ratio of $\text{SiO}_2/\text{Al}_2\text{O}_3$ by weight in the source material. The investigated range of R was 1.42–3.6. Nine concrete geopolymer mixes with R in the above range represent the experimental part carried out. The targeted properties were compressive, splitting, and flexural strengths. The experimental results showed that the R ratio significantly influences the mechanical performance of the final product. The compressive strength improved by 82, 86, 93, and 95%, when metakaolin content was partially replaced by fly ash and GGBS by percentages of 37, 70, 90, 72, and 95% for mixes 2, 3, 5, 7, and 8 respectively. Also, when GGBS partially replaced fly ash content by 36% and 100% for mixes 6 and 9, compressive strength improved by 10.6% and 41.8%, respectively, compared to mix4. Furthermore, the statistical study revealed that the R ratio might be utilized to determine geopolymer strength with reasonable accuracy. The built models were developed by linear and non-linear regression analysis using SPSS software, version 25.

Keywords: Geopolymer Concrete; Fly Ash; Ground Granulated Blast Furnace Slag; Metakaolin; Alkaline Activator; Oven Curing.

1. Introduction

Geopolymer Concrete (GPC) is a form of inorganic polymer composite that has recently emerged as a promising binding medium based on new engineering material usage. By replacing or supplementing traditional concrete, it has the potential to be a significant component of an ecologically sustainable construction sector [1]. The global cement sector generates around 1.35 billion tons of greenhouse gases every year, accounting for about 6-8 % of all artificial greenhouse gas emissions into the atmosphere [2]. Compared to present levels, it is estimated that producing Portland cement will result in a 56.7% rise in CO_2 emissions by 2030 [3]. As a result, new binders are being investigated to replace Portland cement to safeguard the global environment from the effects of cement manufacture [4]. In this regard, geopolymer concrete is one of the most revolutionary developments in new materials in recent history. It can significantly cut CO_2 emissions from the cement industry, which is a good thing. Davidovits was the first scientist to

* Corresponding author: waleed.a.abbas@uotechnology.edu.iq

 <http://dx.doi.org/10.28991/CEJ-2022-08-03-04>



© 2022 by the authors. Licensee C.E.J, Tehran, Iran. This article is an open access article distributed under the terms and conditions of the Creative Commons Attribution (CC-BY) license (<http://creativecommons.org/licenses/by/4.0/>).

adopt the word "geopolymers" and create "geopolymer technology" in 1979. Davidovits proposed that strong alkaline solutions like sodium hydroxide, NaOH, potassium hydroxide, KOH, sodium silicate, Na_2SiO_3 , or potassium silicate, K_2SiO_3 , could be used to react with aluminosilicate-reactive material by dissolving the oxide minerals from the silica-alumina oxides and then poly-condensation to form the final stable silico-aluminate product [5].

Geopolymerisation is an inorganic polycondensation process that involves the rapid reaction at room temperature or at an oven temperature range of 45-80°C to get the hardening of materials containing silica and alumina compounds as a source of aluminosilicate with an alkali metal hydroxide/silicate activator solution, resulting in the formation of a material with a three-dimensional polymeric chain and ring structure, a network structure consisting of Si-O-Al-O bonds [6]. Duxson & Provis [7] found a ternary link between the strength of their respective binder systems and the total Al, Si, and network modifier cation content of the source materials. This ternary diagram was created by analyzing the bulk chemical compositions of aluminosilicate raw materials and ground granulated blast furnace slag. They observed that aluminosilicate sources with lower network modifier concentrations (Ca and Mg) are more likely to generate low-strength geopolymer binders. However, it was observed that not all alumina-silica source materials followed this pattern. While the study discovered some general ways, it did not establish any firm limits for the chemical compositions of bulk aluminosilicate source materials or metakaolin feedstock material that is entirely amorphous and reactive. De Silva et al. [8] showed that systems with a molar ratio of $\text{SiO}_2/\text{Al}_2\text{O}_3$, R, of 3.4–3.8, exhibited a distinctive increase in strength. Duxson et al. [9] also showed that comparable ratios might achieve maximal strength in Metakaolin systems. Fletcher et al. [10] studied varied $\text{SiO}_2/\text{Al}_2\text{O}_3$ ratios in Metakaolin-based geopolymer systems ranging from 0.5 to 300. They determined that the best ratio for strong growth is $\text{SiO}_2/\text{Al}_2\text{O}_3 = 2$. Furthermore, they discovered that geopolymer binder phases with a lower $\text{SiO}_2/\text{Al}_2\text{O}_3$ (<2) ratio or a ratio of $\text{SiO}_2/\text{Al}_2\text{O}_3$ exhibited a weak structure composed of numerous distinct components. Additionally, geopolymer combinations with a high Si content consumed more water, resulting in the formation of hydrated Al species with octahedral coordination. Recently, Autef et al. [11] established that the rate of geopolymerization rises as the amount of quartz SiO_2 in the system decreases. Despite this discovery, they observed total involvement of amorphous silica in the process, allowing the geopolymer network to grow ultimately. Additionally, they discovered that the ideal $\text{SiO}_2/\text{Al}_2\text{O}_3$ ratios for metakaolin-based geopolymers are between 3 and 3.6.

Numerous further papers demonstrate that it is crucial to consider the total SiO_2 and Al_2O_3 concentrations in the feedstock and the reactive content of these oxides [12, 13]. van Jaarsveld et al. [14] proved that fly ashes with a high amorphous content had better mechanical characteristics in binders. In contrast, Brouwers et al. [15] confirmed that the SiO_2 and Al_2O_3 dissolution rates in aluminosilicate material are related to the fly ash glass concentration. Pietersen et al. [16] investigated the reactivity of fly ash during cement hydration. They determined that the ratio of network-forming oxides ($\text{SiO}_2 + \text{Al}_2\text{O}_3 + \text{Fe}_2\text{O}_3$) to network-modifier oxides ($\text{Na}_2\text{O} + \text{K}_2\text{O} + \text{CaO} + \text{MgO}$) in the fly ash glass structure should be between 4 and 9 to achieve optimal reactivity. Similarly, Chen-Tan et al. [17] demonstrated that not all amorphous SiO_2 and Al_2O_3 in fly ash-based Geopolymer systems were involved in the process. Furthermore, they showed that, although complete dissolution of all amorphous SiO_2 and Al_2O_3 phases is not needed, the quality of the end product may be improved if the aluminosilicate source material has a significant percentage of amorphous silica and alumina phases.

On the other hand, Fernández-Jiménez et al. [18] investigated three varieties of fly ash. They concluded that the fly ash with the lowest reactive Al_2O_3 concentration (12.6 percent) had the most insufficient mechanical strength (31 MPa after seven days) when compared to other ash types with a more excellent reactive Al_2O_3 content (18.04 and 22.46 percent). Additionally, Williams & Van Riessen [13] examined the reactive component of fly ash using XRD and XRF methods. They synthesized Geopolymer binders from three distinct fly ashes with $\text{SiO}_2/\text{Al}_2\text{O}_3$ molar ratios of 3.4, 3.4, and 9. They found that Geopolymer binders with a ratio of 3.4 were substantially more potent than those with a ratio larger than 9, but that mixes with a ratio greater than 9 were significantly weaker. While these previous studies demonstrate that the raw material's amorphous SiO_2 and Al_2O_3 phases remain critical for Geopolymer synthesis, there is still some debate regarding the significance of the relationship between total and amorphous phases concerning the $\text{SiO}_2/\text{Al}_2\text{O}_3$ ratio during Geopolymer synthesis. Thus, the current study will investigate the link between the active (amorphous) SiO_2 and Al_2O_3 content of source materials and the strength development of Si-rich Geopolymer systems, relying heavily on previously published data. Many investigations on these systems have been undertaken in Iraq, examining these materials' production methods, processing, characteristics, and uses. Al-Shathr et al. (2016) and Shamsa et al. (2018) investigated the mechanical, curing, and durability properties of GPC and discovered that Geopolymer systems composed of alkaline aluminosilicates had generated considerable interest due to their potentially remarkable mechanical properties, excellent fire performance, good acid resistance, low creep, and low shrinkage [19, 20]. Mathematical modeling is a simplified depiction of reality used to achieve a specific goal. Interacting with models is preferable to dealing with the actual world for various reasons. The motive is often economical to save money, time, or another essential resource [21].

This part of the work aims to build a specified statistical model for predicting compressive strength for Geopolymer concrete that is produced in Iraq, By elucidating the unique chemistry involved in the formation of $\text{SiO}_2/\text{Al}_2\text{O}_3$ GPC, commonly referred to as poly(sialate) Geopolymers, as well as to investigate the effect of R ratio (1.42-3.6) on strength development when ternary and binary binder materials are used to meet the requirements for fresh and hardening properties of GPC, as these parameters are known to have a significant effect. Also, statistical models were built to predict the strength development of Geopolymer concrete.

2. Research Methodology

The flowchart of the research methodology is presented in Figure 1.

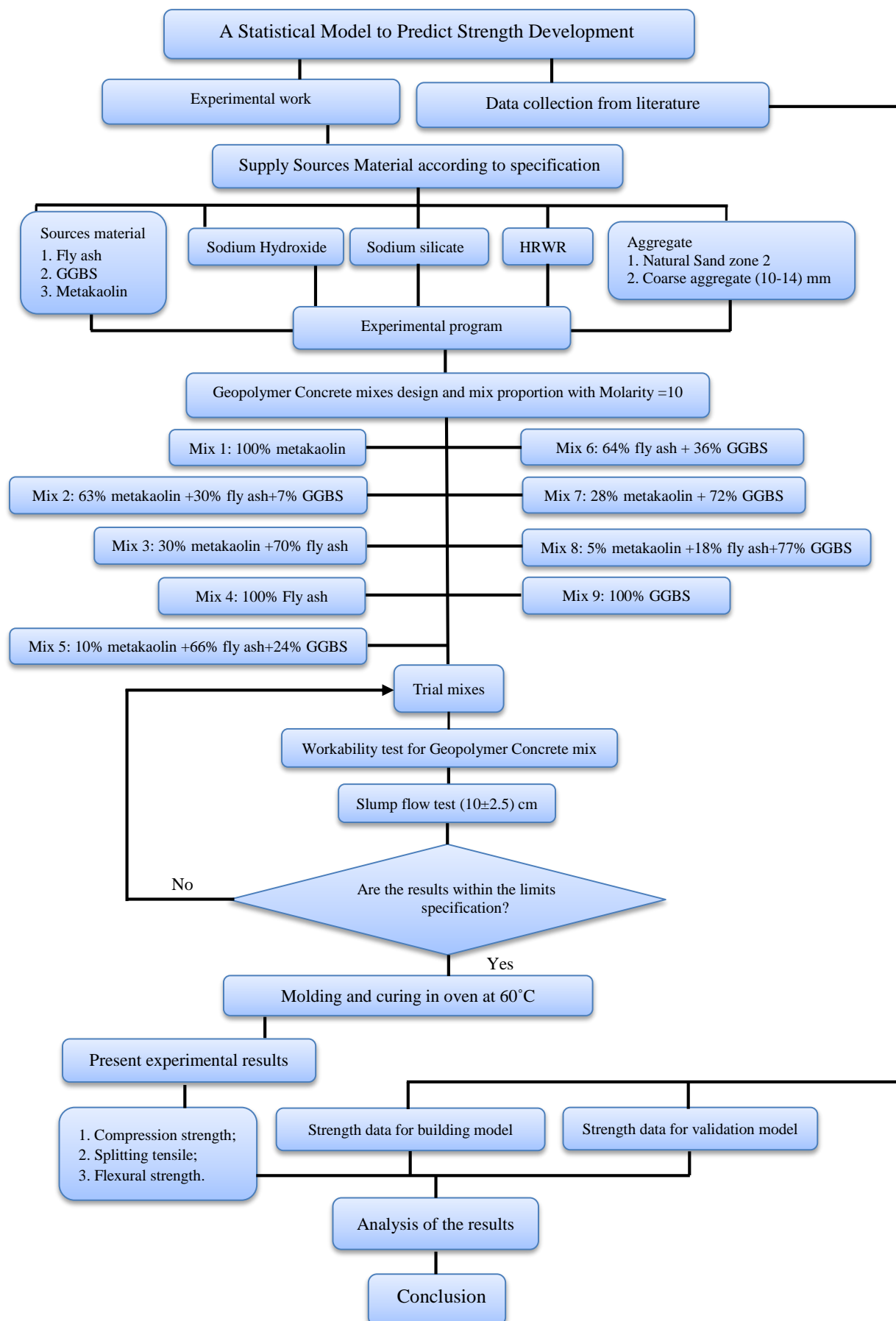


Figure 1. Experimental program used during this investigation

3. Experimental Program

3.1. Used Materials

The materials employed in this investigation were Metakaolin, fly ash, ground granulated blast furnace slag (GGBS), fine aggregates, coarse aggregates, superplasticizer, alkaline solution, and water. The chemical and physical properties of these types of source material are listed in Tables 1 and 2.

Table 1. Oxides content of source materials

Oxides (% by mass)	Fly ash	Metakaolin	GGBS
SiO ₂	61.21	57.04	37.2
Al ₂ O ₃	27.02	39.96	10.31
Fe ₂ O ₃	4.423	1.806	0.9223
CaO	0.00272	0.5936	39.37
MgO	0.2938	0.2142	6.149
SO ₃	0.1297	0.24	0.6
Na ₂ O	0.179	0.078	0.8
Chloride values	0.00837	0.02825	0.03
Others	6.73341	0.03995	4.6187

Table 2. Physical properties of source materials

Physical properties	Fly ash	Metakaolin	GGBS
Loss on ignition, %	0.68	6.12	0.00-2.00
Specific surface area, m ² /kg	3052	4547	5800-6100
Specific gravity	2.12	2.66	2.98
Effective diameter, nm	1687.1	1610.3	278.1

Al-Ukhaider local sand was used as a fine aggregate. It was confirmed to the Iraqi Standard IQS45/1984 [22]. This aggregate has fineness modulus, SSD specific gravity, sulfate content, and absorption of 2.544, 2.6, 0.19%, and 0.75 %, respectively. The used coarse aggregate was crushed gravel of nominal maximum size of 14 mm. It was conforming to the IQS 45/1984 [22]. The crushed gravel has a unit weight, SSD specific gravity, sulfate content, and absorption of 1450 kg/m³, 2.64, 0.096%, and 0.7%, respectively. Figures 2-a and 2-b show the fine and coarse aggregate grading curves, respectively.

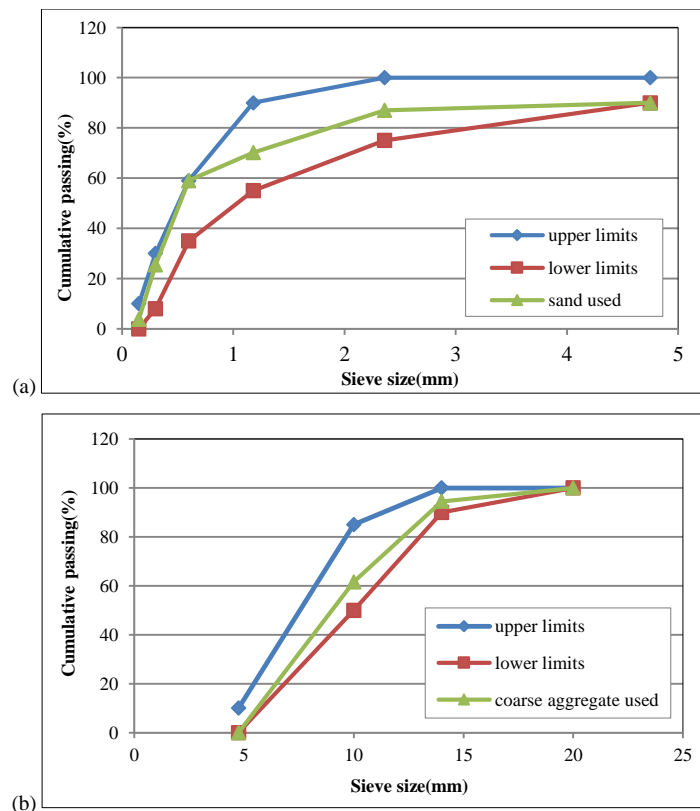


Figure 2. (a) The grading curve for fine aggregate (b) The grading curve for coarse aggregate

Sulphonated naphthalene formaldehyde-based high-range water reducer, Flocretes SP33, was utilized to enhance the fresh GPC workability. This admixture complies with ASTM C494, Type A, and F. [23]. Sodium silicate, Na_2SiO_3 , and sodium hydroxide, NaOH , in pellets with a purity of 99.5%, were used as alkaline activators. The alkaline solution was prepared using portable water

3.2. Geopolymer Concrete Mixes

There is no standard mix proportioning procedure for Geopolymer concrete mixtures. Some basic principles for proportioning heat-cured low calcium fly ash-based Geopolymer concrete. Anyway, most of proportioning is done according to trials. In this study, several attempts of experimental mixes that performed satisfactorily in workability and strength were considered candidate mixes. After several trials mixes, the reference Geopolymer concrete mix was determined to achieve a minimum compressive strength of 30 to 40 MPa at 28 days. Nine GPC mixes with 404 kg/m^3 binder content were cast to investigate the influence of R on strength development, as shown in Figure 3. Heat curing temperatures were varied depending on the type of source material employed. A temperature of 45°C [24] was the highest for Metakaolin. Meanwhile, the GGBS and fly ash-based geopolymer concrete were cured at 60°C [25], as shown in Figure 3. Table 3 shows the details of the reference mix of Geopolymer concrete, and Table 4 lists the R values of the nine mixes.

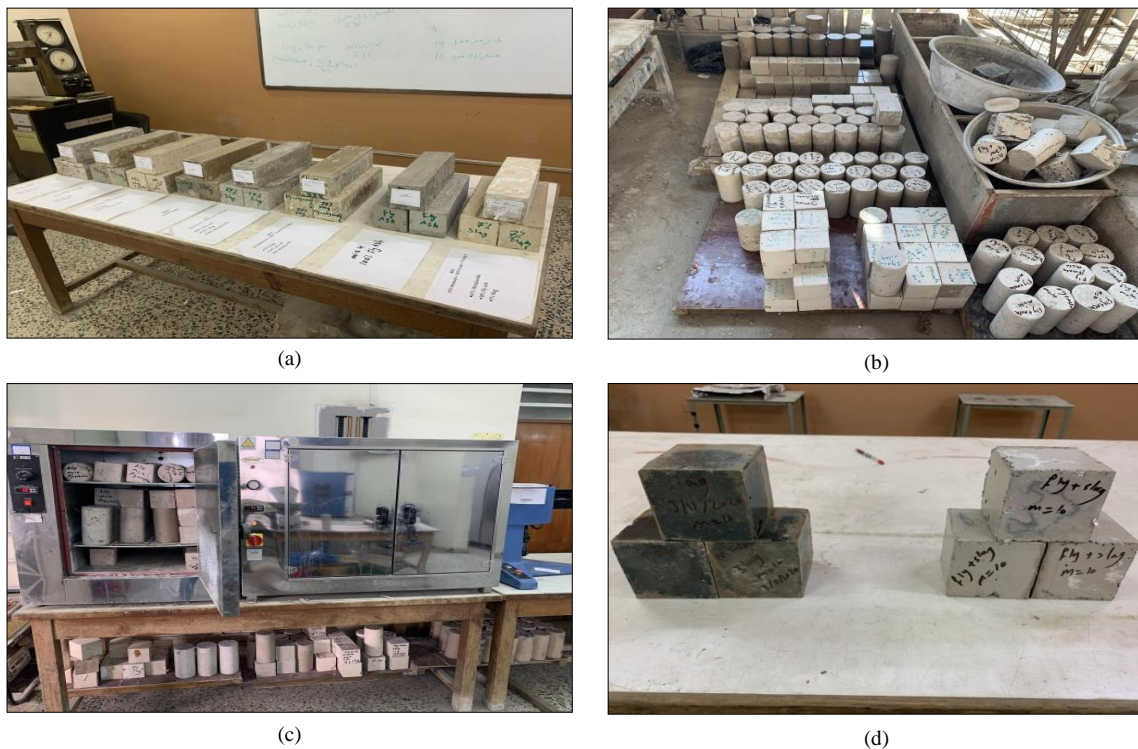


Figure 3. (a, b, c and d) GPC specimen

Table 3. Details of reference mix

Materials	Amount required
NaOH pellets, kg/m^3	26.88
Sodium Silicate solution, kg/m^3	121.88
Water in NaOH solution, kg/m^3	53.49
Na_2SiO_3 / NaOH solution	1.5
water / binder	0.36
activator solution / binder	0.55
Extra water, kg/m^3	15.61
Fine aggregate, kg/m^3	700
Coarse aggregate, kg/m^3 :	1100
a) size 5-10mm	660
b) size 10-14mm	440

Table 4. Values of R

Mix	1	2	3	4	5	6	7	8	9
FA, %	0	30	70	100	66	64	0	18	0
Mk, %	100	63	30	0	10	0	28	5	0
GGBS, %	0	7	0	0	24	36	72	77	100
R	1.42	1.82	2.01	2.26	2.5	2.74	2.99	3.25	3.6

4. Results and Discussion

4.1. Effect of R on Strength Development

4.1.1. Compressive Strength

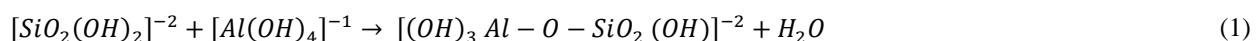
Table 5 lists the compressive strength (f_c) for the investigated mixes at 7 and 28 days. The compressive strength values at the 28-day were not considerably higher than at the 7-day. That suggests that most of the geopolymerization process in the system was almost finished by the 7th day. The test results demonstrated that changing the R ratio positively influences the compressive strength of Geopolymers [26]. When metakaolin content was partially replaced by fly ash and GGBS in mixes 2, 3, 5, 7, and 8, compressive strength improved by 82%, 86%, 93%, and 95%, respectively to mix1. This is due to amorphous oxides in the source material, which contributed to the increased compressive strength [27]. When fly ash content was fully or partially replaced by GGBS in mixes 6 and 9, compressive strength improved by 10.6% and 41.8%, respectively, when compared to mix 4. The high compressive strength of GGBS mixes can be linked to the robust load-bearing gel structure that develops in the binder regions. In addition, the mechanisms of dissolution and precipitation in these systems are based on alkali-mediated dissolution and precipitation mechanisms in their early stages [25]. Activator concentrations give the system enough alkalinity to develop and maintain a high pH, promoting silica and alumina breakdown from the GGBS. Together with calcium, which is insoluble at increased pH but is liberated along with the silicate and aluminate species when the alkali attacks the slag particles, these dissolved species subsequently precipitate and function as nucleation nuclei, supporting the development of calcium silicate hydrate gel. Also, the presence of CaO in GGBS has a significant role in increasing the compressive strength of the slag-based GPC [15, 16].

Table 5. Strength development of investigated Geopolymer mixes

Mix	R	Compressive strength, MPa		Splitting tensile strength, MPa	Flexural strength, MPa
		7 days	28 days	28-day	28-day
1	1.42	2.7	3.0	0.35	0.76
2	1.82	16.0	17.5	1.20	1.90
3	2.01	21.3	22.7	1.85	2.44
4	2.265	40.5	45.5	2.50	3.50
5	2.50	44.1	46.0	2.90	4.07
6	2.74	45.3	50.9	3.13	4.25
7	2.99	56.0	64.8	3.21	4.30
8	3.25	71.5	72.5	3.25	4.65
9	3.60	77.4	78.2	4.00	5.30

On the other hand, the hardening of specimens happens due to geopolymerization reactions, which involve intensification interacting that differ depending on the kind of aluminate and silicate used, which result in the formation of silicate and aluminate monomers. $[Al(OH)_4]^{-1}$, $[SiO(OH)_3]^{-1}$, and $[SiO_2(OH)_2]^{-2}$ the silicate and aluminate monomers formed as a result of the hydrolysis interaction or dissolution of Al^{+3} and Si^{+4} Components. In this method, the concentration of NaOH solution employed as the activator solution impacts the result. At high intensification of NaOH (10 molar), the early stages of the intensification interact, beginning with the creation of a stable oligomer as a dimer as a result of intensification between $[Al(OH)_4]^{-1}$ and $[SiO_2(OH)_2]^{-2}$ As shown in Equation 1, they can be observed as stable oligomers. The resulting structure is as follows:

Equation 1 is a settled dimer structure within the structure of polysialat (Si: Al = 1).



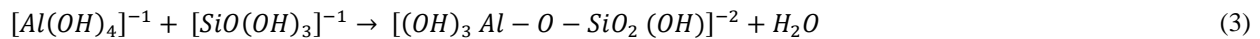
When the Si/Al ratio is low, one factor contributing to the delay of the polymerization practical is the low compressive strength.

This state, simply known as the early high dissolution of Al, occurred in a relatively short period. Low quantities of Si (a low Si/Al ratio) result in the formation of a poly(sialate) structure [28]. At low Si/Al ratios, the $[\text{Al}(\text{OH})_4]^{-1}$ monomer makes up the majority of the aluminum, indicating that the aluminum is not oxidized. Because of the high concentration of $[\text{Al}(\text{OH})_4]^{-1}$ monomer, the alkalinity of the reaction product in Equation 1 is high, and the reaction product tends to react with $[\text{Al}(\text{OH})_4]^{-1}$ resulting in the formation of an aluminosilicate trimer [29]. However, even though this sort of dimer and trimer was the most abundant, greater polymerization is complex under these conditions, which causes the geopolymer's hardening process to be disrupted. Aluminate is readily generated in high aluminate, resulting in a weaker link than the bond formed by SiO-Al in a Geopolymer system. The link between Si-O-Si is theoretically stronger than the bonds between Si-O-Al and Al-O-Al, which means that the strength of the bond grows as the Si/Al ratio increases [29].

Because of the high aluminate content in the system, the low Si/Al ratio affects the loss of compressive strength linked with the low $[\text{SiO}(\text{OH})_3]^{-1}$ structure, resulting in the formation of a bigger Geopolymer structure than the $[\text{SiO}_2(\text{OH})_2]^{-2}$ Structure as a result. It is important to note that the pH affects both kinds of silicate structures [30]. The Si speciation diagram Figure-5 indicates that the structure of $[\text{SiO}(\text{OH})_3]^{-1}$ is more settled than the structure of $[\text{SiO}_2(\text{OH})_2]^{-2}$ under high alkaline conditions.

According to the reaction in Equation 2 [30], increasing the ratio of Si to Al is beneficial to supply an additional silicate component in the form of $[\text{SiO}(\text{OH})_3]^{-1}$ monomer.

Availability $[\text{SiO}(\text{OH})_3]^{-1}$ with $[\text{Al}(\text{OH})_4]^{-1}$, the monomer completes the condensation reaction (Equation 3) and self-polymerization between silicate groups formed during silicate oligomer formation.



Further condensation between the reaction product (Equation 3) and $[\text{SiO}(\text{OH})_3]^{-1}$ to generate more stable products is carried out until all of the $[\text{Al}(\text{OH})_4]^{-1}$ monomer employed in the interaction. Whenever there is a high concentration of Si in a system (i.e., when the Si/Al ratio is high), the condensation process begins with creating oligomer silicates. [25] Finally, the composition of the construction of a polymer network is completed.

The interaction carries on until Geopolymer(GP) structures of poly(sialate-siloxo), -Si-O-Al-O-Si-O- or poly(sialate-disiloxo), -Si-O-Al-O-Si. The higher the intensification of the dissolved silicate source, the more Si-O-Si bonds and compressive strength [31]. Furthermore, the creation of a Geopolymer network is dependent on the concentration of $[\text{SiO}(\text{OH})_3]^{-1}$. When the Si/Al ratio is low, the resulting silicate monomer is $[\text{SiO}_2(\text{OH})_2]^{-2}$ and $[\text{Al}(\text{OH})_4]^{-1}$. The intensification process between the two forms tiny oligomers such as dimers and trimers [29]. The concentration of $[\text{SiO}(\text{OH})_3]^{-1}$ rose with increasing Si/Al ratio, where the condensation reaction between $[\text{SiO}(\text{OH})_3]^{-1}$ and $[\text{Al}(\text{OH})_4]^{-1}$ forms large oligomers and leads to the formation of a tangly polymer network, thereby improving the strength. The specific surface area and particle size distribution of source material impact the compressive strength of binder-based Geopolymers. In most cases, increased compressive strength values are finer particle size; this may be due to the greater area available for leaching and activation, creating Geopolymer gel. It is generally known that spherical fly ash granules contribute to better workability while using the least alkaline liquid. Still, the Metakaolin plate shape requires a larger volume of solution to provide superior homogeneity and strength [20].

4.1.2. Splitting Tensile Strength

Splitting tensile strength of Geopolymer concrete with various replacements of GGBS were performed, and the results have been summarized in Table 5. The results showed that the splitting tensile strength increases with an increase in the R ratio. The maximum splitting tensile strength was obtained for mix 9 with 100% GGBS than another mix. It was observed that when the replacement percentage of GGBS by fly ash, Metakaolin, or both increases, the concrete's tensile strength also increases. The percentage of increase in tensile strength 13.7%, 20.12%, 23%, and 37.5% for mix 5, 6, 8 and 9 respectively when compared with mix 4. Because incongruously, the inclusion of silica raised the R ratio, which impeded the Geopolymer reactions and subsequent gelation process [32].

On the contrary, the strength will decrease when the replacement portion of Metakaolin by fly ash, GGBS, or both increases. The percentage of decrease in tensile strength 52 and 26 for mix 2, 3 respectively, compared with mix 4. Also, the rate of decreasing in tensile strength 19.75% for mix 8 when compared with mix 9. The higher content of Metakaolin in fly ash and GGBS based Geopolymer concrete caused the mixture to become stickier and take longer to harden. Furthermore, as indicated by Kusbiantoro et al. [33], the higher curing temperature of roughly 60 C° allows for increased solubility of Si and Al ions. Therefore, the production of a stronger polymer chain leads to increase strength.

4.1.3. Flexural strength

Table 5 shows the variation in flexural strength at 28 days. According to the test results, it was recorded that when the percentage of GGBS in the concrete increase, the flexural strength of the concrete increases as well. The increase in

flexural strength was 14%, 17.64%, 24.73%, and 33.96% for mix 5, 6, 8 and 9, respectively, when compared with mix 4. Because incongruously, the inclusion of silica raised the R ratio, which impeded the Geopolymer reactions and subsequent gelation process [32]. On the contrary, the strength will decrease when the replacement portion of Metakaolin by fly ash, GGBS, or both increases. The percentage of decreasing in flexural strength 45.71% and 30.28% for mix 2, 3 respectively when compared with mix 4. Also, the rate of reducing flexural strength was 18.86% for mix 8 when compared with mix 9. This is because a higher silicate content increases the strength of the material since it intensification the microstructure as a result of the high degree of densification. Also, the inclusion of silica resulted in an incongruent increase in the R ratio, which impeded the Geopolymer reactions and subsequent gelation process [34].

4.2. Mathematical Model Building and Statistical Analysis

4.2.1. Data Collection for Building and Validating the Model

In addition to the present work, compressive strength and R data were collected from local and international literature to build and validate the Mathematical Model. These data were divided into two groups. The first group, which contains the information of the 22 compressive strengths, was adopted to build the model. These compressive strengths for this part were divided into fifteen included references, and seven present the current experimental results, as shown in Table 6. The second group, which contains the information of 8 compressive strengths, was selected to test the model's validity. Again, these compressive strengths were divided into six included references and two present experimental results, as shown in Table 7. Linear regression analysis was adopted to build a model that describes the relationship between R and compressive strength. SPSS software, version 25, was used for this mission. Only fly ash, GGBS, and Metakaolin-based Geopolymer concrete mixes have been studied for the sake of clarity. Linear regression analysis was adopted to build a model that describes the relationship between R and compressive strength. SPSS software, version 25, was used for this mission. Only fly ash, GGBS, and Metakaolin-based Geopolymer concrete mixes have been studied for the sake of clarity.

Table 6. The information of the Fifteen included references and seven present experimental results for this part used in model building

No.	Reference	Weight of Binder (kg/m ³)	R1 (%)	Alkaline solution/ binder ratio (kg/m ³)	Coarse aggregate (kg/m ³)	Fine aggregate (kg/m ³)	Compressive Strength (MPa)
1	Present experimental results	404	1.42	0.55	1100	700	3.0
			1.82				17.5
			2.01				22.7
			2.265				45.5
			2.50				46.0
			2.99				64.8
			3.6				78.2
2	Nuruddin et al. [35]	400	2.13	0.5	950	850	37.0
3	Joseph & Mathew [36]	420.57	2.10	0.55	1273	318	37.0
420.57		2.10	0.55	1196	395	38.0	
5	Partha et al. [34]	400	1.76	0.35	1217	655	27.0
6	Noushini & Castel [37]	400	2.01	0.38	1193	672	19.5
7	Samdani & Quadar [38]	360	2.27	0.45	1275	580	35.0
8		440	2.27	0.25	1206	635	37.0
9	Shamsa et al. [20]	400	2.32	0.45	1200	650	46.59
10		414	2.56	0.45	1166	660	35.23
11		414	2.92	0.45	1166	660	49.9
12	Divvala & Rani [39]	414	3.04	0.45	1166	660	55.5
13		420	2.09	0.55	966	810	31.2
14		400	2.09	0.55	966	810	27.8
15	Rao and Rao [40]	456	2.62	0.47	706	872	41.5
16		433.6	2.642	0.47	706	872	39

Table 7. The information of the six included references, and two present experimental results for this part used to validate the model

No.	Reference	Weight of Binder (kg/m ³)	R (%)	Alkaline solution/binder ratio (kg/m ³)	Coarse aggregate (kg/m ³)	Fine aggregate (kg/m ³)	Compressive Strength (MPa)
1	Present experimental results	404	2.74	0.55	1100	700	50.9
		404	3.25	0.55	1100	700	72.5
2	Nguyen et al. [42]	436	2.00	0.45	1308	654	32
3	Ryu et al. [43]	360	2.10	0.4	1047	687	39
4	Albitar et al. [44]	424.8	1.88	0.37	1181	595	19.7
5	Samdani & Quadar [38]	390	2.27	0.35	1287	585	36.0
6	Divvala & Rani [39]	414	2.80	0.45	1166	660	47.4
		414	3.16	0.45	1166	660	60.03

4.2.2. Compressive Strength Model

From Table 6, fifteen actual strength data were selected from references and seven current experimental results of compressive strength to build the mathematic model and determine the accuracy of the correlation between R ratio and compressive strength. Firstly, the fundamental regression analysis was used to determine whether or not there is an impact between compressive strength and R by evaluating the functional connection between the independent and dependent variables.

According to the findings, the relationship between compressive strength and the ratio of R was robust and statistically significant at the 92 percent confidence interval, as shown in Table 8. The link between them is best described by point disruption around a straight line. In this scenario, nearly all of the data fall on both sides of a straight line with a positive (upward) slope, implying that they had a positive association. Therefore, it can be concluded that a strong relationship can be dependent on compressive strength and R ratio [45]. Table 8 shows the Descriptive A NOVA test between variable building data and R. The final model equation is designed to estimate compressive strength (Equation 4). The appropriate line plot for the linear model built is illustrated in Figure 4. The plot also shows the incremental rounding of the parameter on compressive strength.

$$\text{Compressive strength(MPa) at 28 days} = -33.33 + 30.43 \times R1 \quad (4)$$

Table 8. Descriptive model summary, Coefficients, and ANOVA test between variable building data and R

Model summary					
R	R square	Adjusted R square	Std. error of the estimate		
0.923	0.852	0.845	6.378		
The independent variable is R1 from research and present experimental result for building model, (%).					
Coefficients					
	Sum of squares	df	Mean square	F	Sig
R1 from research and present experimental result for building model,(%)	30.427	2.834	0.923	10.736	0.000
Constants	33.327	6.777		-4.918	0.000
ANOVA					
	Sum of square	df	Mean square	F	Sig
Regression	4688.385	1	4688.385	115.260	0.000
Residual	813.533	20	40.677		
Total	5501.918	21			
The independent variable is R1 from research and present experimental result for building model, (%).					

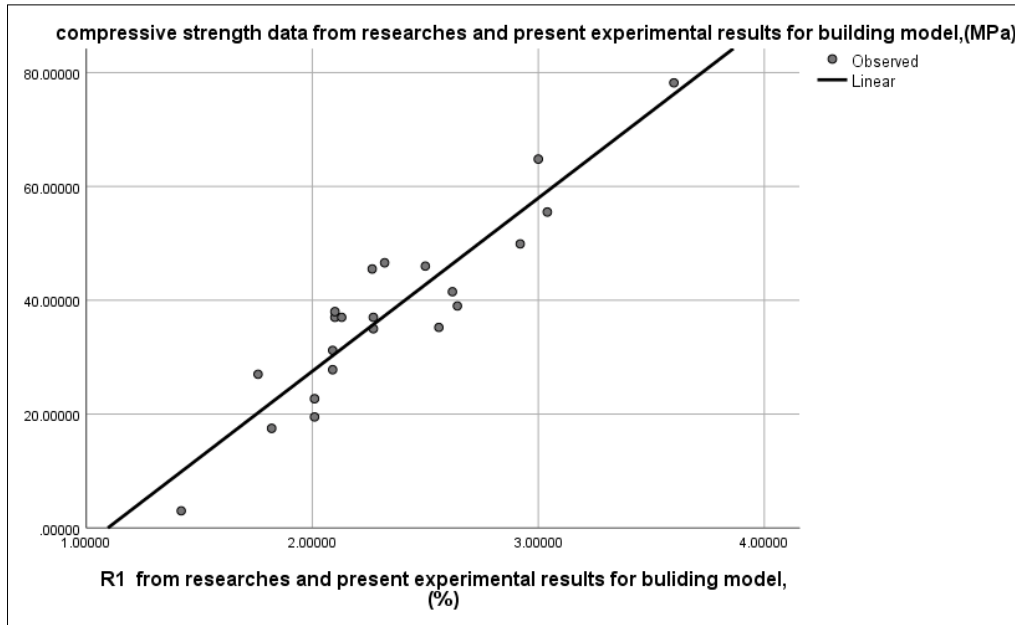


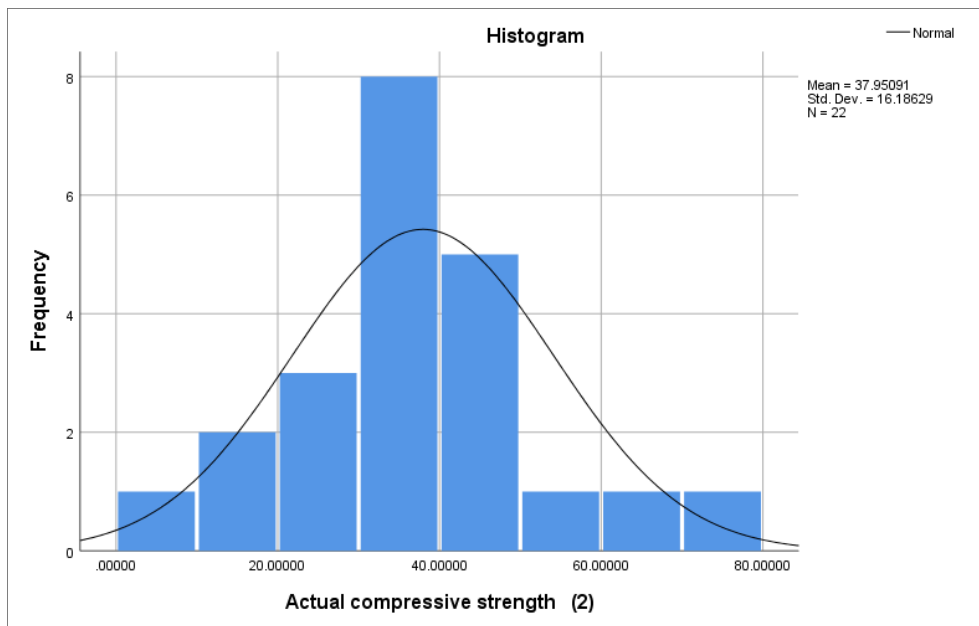
Figure 4. Line the relationship between R and building data for the model

Secondly, the distribution test is used to determine whether that data follow the normal distribution, and therefore, this assumption is met in your data for statistical tests. From Table 9 and Figure 5-a and 5-b we can conclude that the data appears to be normally distributed as it follows the diagonal line closely and does not appear to have a non-linear pattern. Also, Table 9 presents the results tests of normality, and it can be concluded that the test significance of 0.2 is greater than the significance level ($\alpha=0.05$). Then accept the null hypothesis; there is not enough evidence to conclude that the data is non-normal and there is the link between the actual strength and R. Therefore, we can depend on this model in Equation 4 to find a general compressive strength equation.

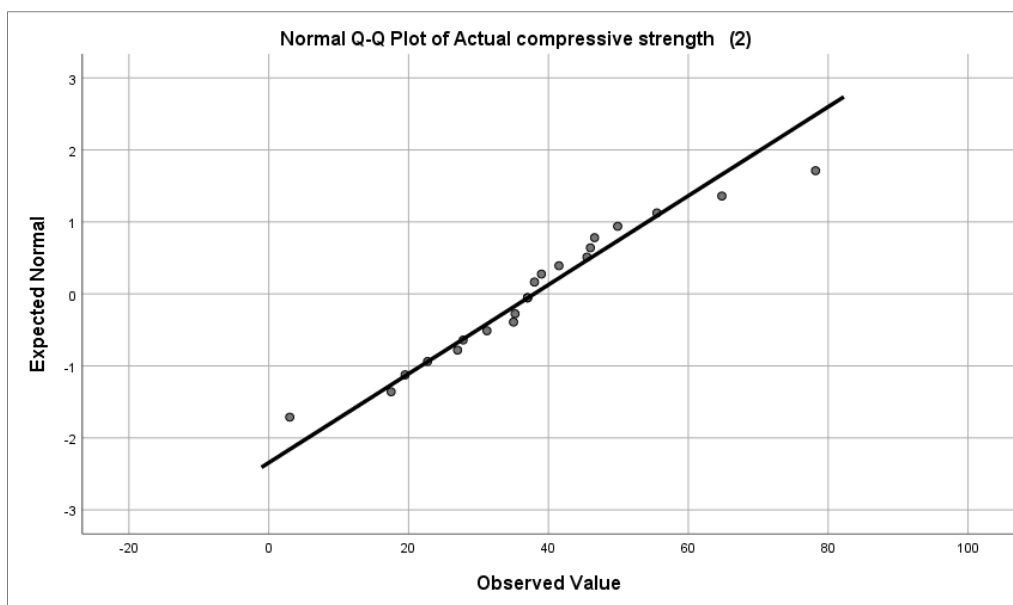
Table 9. Tests of Normality by using Kolmogorov-Smirnov* and Shapiro-Wilk test for Actual compressive strength

	Statistic	df	Sig.	Statistic	df	Sig.
Actual compressive strength	0.115	22	0.200**	0.971	22	0.734

* Lilliefors Significance Correction; ** This is a lower bound of the true significance.



(a)



(b)

Figure 5. (a) and (b) distribution test result

4.2.3. Validation of Compressive Strength Model

Finally, from the Table 7, six actual strength data from included references and two percent experimental results compressive strength were randomly selected to validate the final model Equation 5 by estimating the differences between validation strength and calculated strength (Estimated strength from the model in Equation 1 as shown in Table 10. The result shows a linear relationship between actual compressive strength and estimated compressive strength with a .954 confidence interval, the correlation between them. The link between them is best described by point disruption around a straight line. In this scenario, nearly all of the data fall on both sides of a straight line with a positive (upward) slope, implying that they had a positive association. Therefore, there is a relationship between actual compressive strength and estimated strength [45]. Table 11 shows the Descriptive A nova test between validation strength and Estimated strength. From Figure 6 and Table 10, the final model equation is designed to estimate a general compressive strength (Equation 5).

$$\text{Compressive strength at 28 days} = 1.97 + 0.982 * \text{Estimated strength} \tag{5}$$

Table 10. Calculation of the Estimated strength from the model by the excel program

No.	Reference	Weight of Binder (kg/m ³)	R2 (%)	Actual strength (3)	Estimated strength from model = $-33.33 + 30.43 \times R2$
1	Nguyen et al. [42]	436	2.00	32	27.5300
2	Ryu et al. [43]	360	2.10	39	30.5730
3	Albitar et al. [44]	424.8	1.88	19.7	23.8784
4	Samdani & Quadar [38]	390	2.27	36	35.7461
5	Divvala & Rani [39]	414	2.8	47.4	51.8740
6	Divvala & Rani [39]	414	3.16	60.03	62.8288
7	Present study	400	2.74	50.9	50.0482
8	Present study	400	3.25	72.5	65.5675

Table 11. Descriptive the model summary and ANOVA test between validation strength and Estimated

R	R square	Adjusted R square	Std. error of the estimate		
0.954	0.911	0.896	5.374		
ANOVA					
	Sum of squares	df	Mean square	F	Sig.
Regression	1774.742	1	1774.742	61.443	0.000
Residual	173.306	6	28.884		
Total	1948.048	7			

The independent variable is the Estimation of compressive strength from the model (MPa).

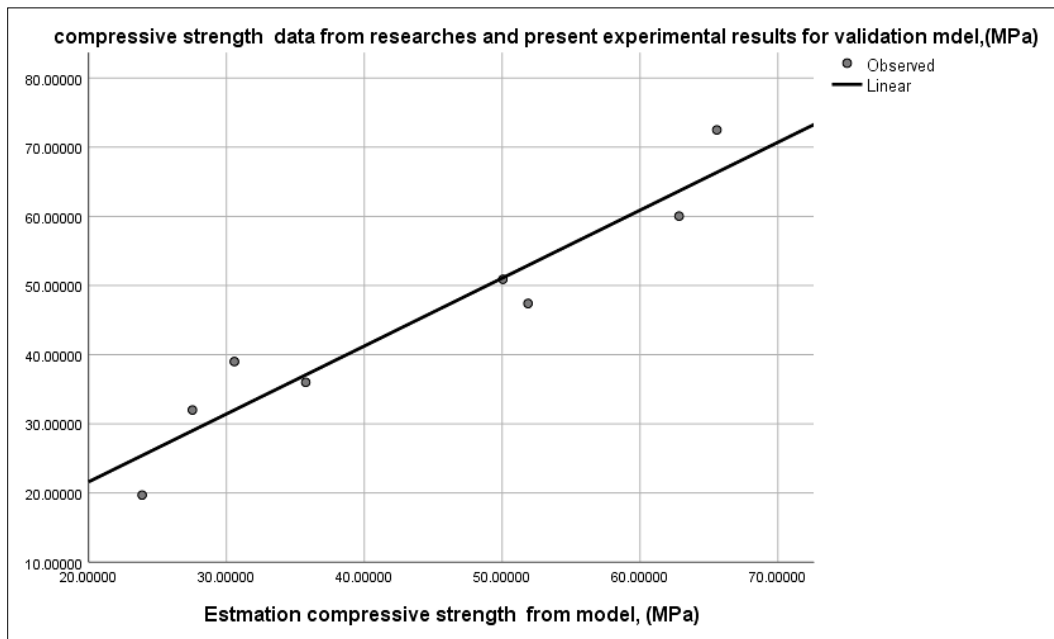


Figure 6. Relationship between validation compressive strength and estimated strength from the model

4.2.4. Relationship Model between Different Types of Strength

Generally, it has been stated that the splitting tensile strength and flexural strength of normal concrete may be determined from compressive strength using numerous empirical relationships proposed by various concrete institutes and academics [46-52]. From Table 12 and Figure 7, it can be concluded the following generic Equation 6 can be used to synthesize these empirical relationships between the compressive strength model and splitting tensile strength model:

$$f'_{ct} = 0.162(f'_c)^{0.731} \tag{6}$$

where f'_{ct} is Splitting strength at 28 days in MPa, and f'_c is the compressive strength in MPa. The relationship between the f'_c model and f'_{ct} model for experimental data is a present illustration in Figure 4.

Table 12. Model Summary and Coefficients between the compressive strength and Split Tensile Strength model for experimental data present

Model summary					
R	R Square	Adjusted R Square	Std. Error of the Estimate		
0.992	0.984	0.982	0.102		
The independent variable is the present experimental result compressive strength					
Coefficients					
	Sum of squares	df	Mean square	F	Sig.
Compressive strength from present experimental result (MPa)	0.731	0.035	0.992	20.948	0.000
(constant)	0.162	0.020		7.897	0.000
The dependent variable is in (splitting tensile strength)					
NOVA					
	Sum of square	df	Mean square	F	Sig.
Regression	4.546	1	4.546	438.803	0.000
Residual	0.073	7	0.100		
Total	4.619	8			
The independent variable is the present experimental result compressive strength					

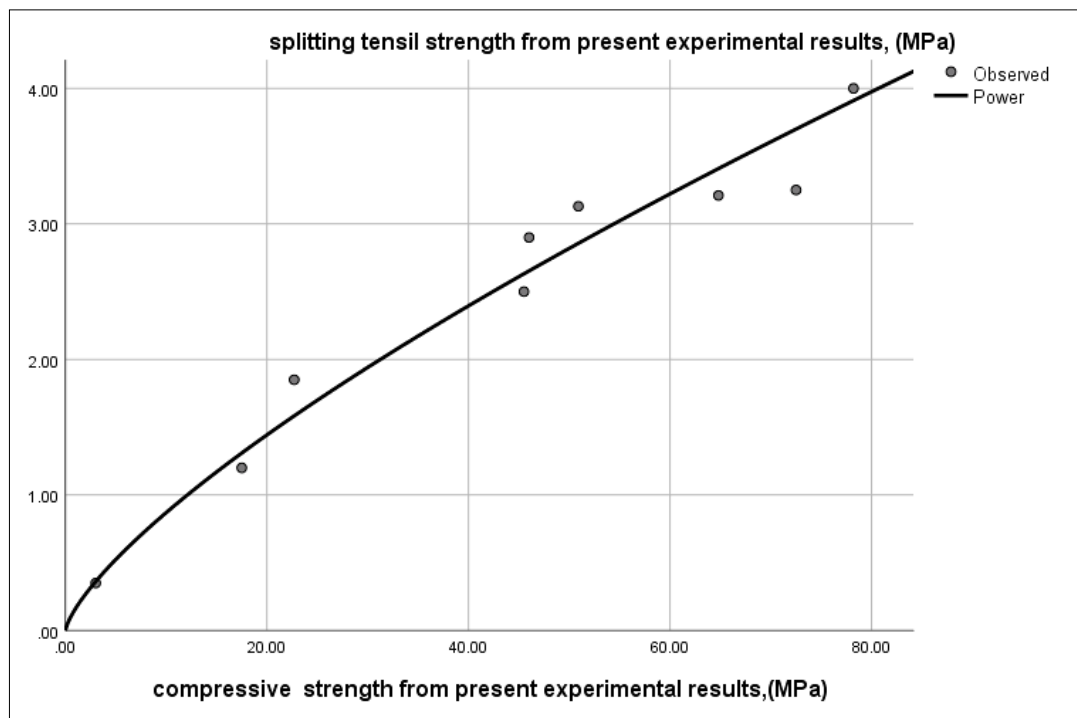


Figure 7. Relationship between the f'_c model and f'_{ct} model for experimental data present

From Table 13 and Figure 8, it can be concluded generic Equation 7 summarizes the empirical relationships between compressive and flexure strength for Geopolymer:

$$f'_{cf} = 0.384(f'_c)^{0.592} \tag{7}$$

where f'_{cf} is flexural strength at 28 days in MPa and f'_c is compressive strength in MPa.

Table 13. Model Summary, Standardized Coefficients, and ANOVA between the compressive and flexural strength models for experimental data present

Model Summary					
R	R Square	Adjusted R Square	Std. Error of the Estimate		
0.994	0.989	0.987	0.070		
The independent variable is the present experimental result compressive strength.					
Coefficients					
	Sum of squares	df	Mean square	F	Sig.
Compressive strength from present experimental result, (MPa)	0.592	0.024	0.994	24.734	0.000
(Constant)	0.384	0.033		11.509	0.000
The dependent variable is in (Flexural strength (MPa)).					
ANOVA					
	Sum of squares	df	Mean square	F	Sig.
Regression	2.984	1	2.984	611.760	0.000
Residual	0.034	7	0.005		
Total	3.018	8			
The independent variable is the present experimental result compressive strength.					

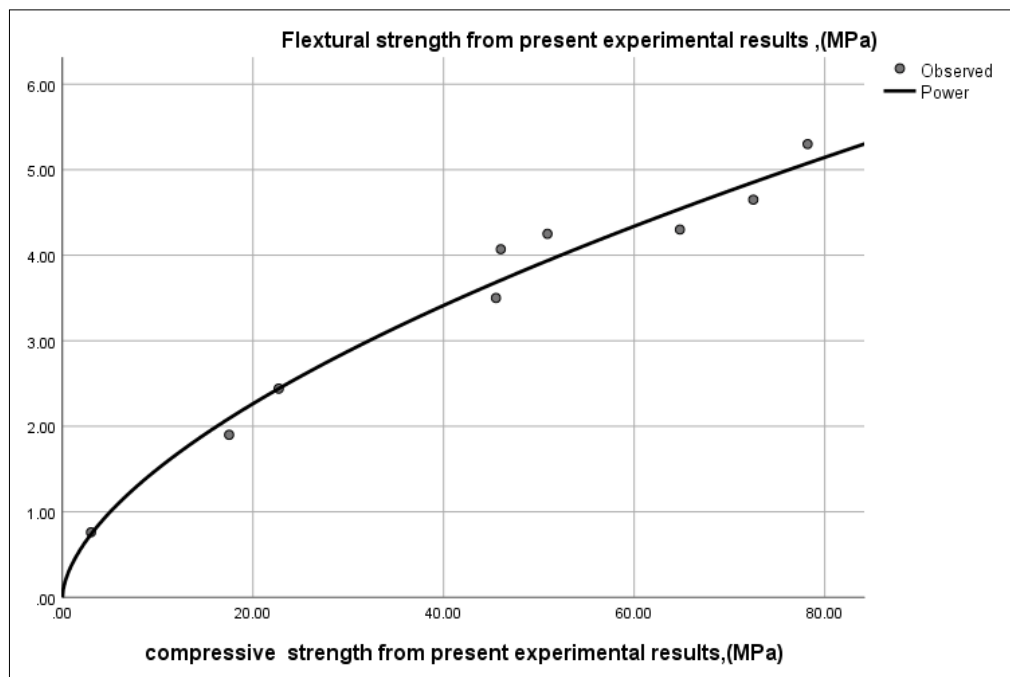


Figure 8. Relationship between the compressive and flexural strength models for experimental data present

According to the findings of ACI [53] and Albitar et al. [54], which were obtained from a database of all known experiments on Geopolymer concretes built from Class-F fly ash. Hardjito & Rangan [55], Raijiwala & Patil [56], Nguyen et al. [57], Olivia and Nikraz [58], Ivan Diaz-Loya et al. [59], and Albitar et al. [54] suggested splitting tensile and flexural models are described in Equations 5 and 6, respectively. Mechanical characteristics of fly ash-slag-based Geopolymer concrete are comparable to those of fly ash-based geopolymer concrete. Table 14 shows the comparison between Equations 8 and 9 for the tensile strength by the proposed model of Albitar et al. [54] for splitting tensile strength.

$$f'_{ct} = 0.6 \sqrt{f'_c} \tag{8}$$

The proposed model of Albitar et al. [54] for flexural strength:

$$f'_{cf} = 0.75 \sqrt{f'_c} \tag{9}$$

Table 14. Comparison between Equations 6 and 8 for tensile strength

Equation	Mix No.								
	1	2	3	4	5	6	7	8	9
Actual f'_c from present research	3	17.5	22.7	45.5	46	50.9	64.8	72.5	78.2
Experimentally determined of f'_{ct}	0.35	1.2	1.85	2.5	2.9	3.13	3.21	3.25	4
Predictive Model $f'_{ct} = 0.6 \sqrt{f'_c}$	1.03	2.50	2.85	4.04	4.06	4.28	4.82	5.10	5.30
Predictive Model $f'_{ct} = 0.162(f'_c)^{0.731}$	0.36	1.31	1.58	2.63	2.66	2.86	3.41	3.71	3.92

Also, Table 15 shows the comparison between Equations 7 and 9 for flexural strength proposed model of Albitar et al. [54] for flexural strength.

Table 15. Comparison between Equations 7 and 9 for flexural strength

Equation	Mix No.								
	1	2	3	4	5	6	7	8	9
Actual f'_c from present research	3	17.5	22.7	45.5	46	50.9	64.8	72.5	78.2
Experimentally Determined of f'_{cf}	0.76	1.9	2.44	3.5	4.07	4.25	4.3	4.65	5.3
Predictive Model $f'_{cf} = 0.75 \sqrt{f'_c}$	1.29	3.13	3.57	5.05	5.08	5.35	6.03	6.38	6.63
Predictive Model $f'_{cf} = 0.384(f'_c)^{0.592}$	0.73	2.09	2.44	3.68	3.71	3.94	4.54	4.86	5.08

From Tables 14 and 15, the experimentally determined values of splitting tensile and flexural strength were less than those in the expressions prescribed by ACI [53] and Albitar et al. [54], indicating that binder-based geopolymer concrete exhibits less tensile strength and flexural strength than Albitar et al.'s finding.

5. Conclusions

The following conclusions are drawn from the experimental inquiry:

- The compressive strength improved by 82, 86, 93, and 95%, when Metakaolin content was partially replaced by fly ash and GGBS by percentages of 37, 70, 90, 72, and 95% for mixes 2, 3, 5, 7, and 8 respectively. Also, when GGBS partially replaced fly ash content by 36% and 100% for mixes 6 and 9, compressive strength improved by 10.6% and 41.8%, respectively, compared to mix 4.
- The statistical analysis reveals that the synergistic effect of the linear term of the R ratio has a considerable impact on early compressive strength.
- The statistical analysis revealed that the R ratio might be utilized to assess geopolymer strength accurately. Furthermore, the R ratio, rather than the NaOH/Na₂SiO₃ ratio, significantly impacts strength development.
- The compressive strength, flexure strength, and splitting tensile strength of geopolymer concrete improve when the concentration of sodium hydroxide and the ratio of R increase in terms of molarities of sodium hydroxide and the percentage of R. The compressive strength of the geopolymer concrete increases when the curing period is extended. The gain in strength after 24 hours, on the other hand, is statistically significant.
- The presence of CaO in GGBS has a significant role in increasing the compressive strength of the slag-based GPC and the high aluminate content in the system, and the low Si/Al ratio affects the loss of compressive strength.
- With an increase in the mass ratio of water to GPC by mass, the compressive strength of the geopolymer concrete drops as well.
- Using fly ash, Metakaolin, and GGBS as fillers or replacements in GPC concrete will help prevent environmental pollution because they cause agricultural land to be changed into barren land when they are disposed of as garbage.
- A mixture containing 72 % GGBS and 30 % metakaolin appears to have greater compressive strength than other mixtures, including Metakaolin. According to some theories, this is due to an increase in the alkaline interaction between the GGBS particles and the calcium in Metakaolin. Also, the compressive strength, flexure, and tensile strength of geopolymer concrete increased with the increase of slag content.

6. Declarations

6.1. Author Contributions

Conceptualization, T.S.A., and W.A.A.; methodology, T.S.A., and W.A.A.; software, A.A.A.; validation, T.S.A., and W.A.A.; formal analysis, A.A.A.; investigation, A.A.A.; resources, A.A.A.; data curation, A.A.A.; writing—original draft preparation, A.A.A.; writing—review and editing, T.S.A., and W.A.A.; visualization, A.A.A.; supervision, T.S.A., and W.A.A.; project administration, T.S.A., W.A.A., and A.A.A. All authors have read and agreed to the published version of the manuscript.

6.2. Data Availability Statement

The data presented in this study are available in the article.

6.3. Funding

The authors received no financial support for the research, authorship, and/or publication of this article.

6.4. Conflicts of Interest

The authors declare no conflict of interest.

7. References

- [1] Davidovits, J. (1991). Geopolymers - Inorganic polymeric new materials. *Journal of Thermal Analysis*, 37(8), 1633–1656. doi:10.1007/BF01912193.
- [2] Hardjito, D., Wallah, S. E., Sumajouw, D. M. J., & Rangan, B. V. (2005). Fly Ash-Based Geopolymer Concrete. *Australian Journal of Structural Engineering*, 6(1), 77–86. doi:10.1080/13287982.2005.11464946.
- [3] Sanjuán, M. Á., Andrade, C., Mora, P., & Zaragoza, A. (2020). Carbon Dioxide Uptake by Cement-Based Materials: A Spanish Case Study. *Applied Sciences*, 10(1), 339. doi:10.3390/app10010339.

- [4] Mehta, A., & Siddique, R. (2017). Properties of low-calcium fly ash based geopolymer concrete incorporating OPC as partial replacement of fly ash. *Construction and Building Materials*, 150, 792–807. doi:10.1016/j.conbuildmat.2017.06.067.
- [5] Schmücker, M., & MacKenzie, K. J. D. (2005). Microstructure of sodium polysialate siloxo geopolymer. *Ceramics International*, 31(3), 433–437. doi:10.1016/j.ceramint.2004.06.006.
- [6] Van Chanh, N., Trung, B. D., & Van Tuan, D. (2008). Recent research geopolymer concrete. In *The 3rd ACF International Conference-ACF/VCA, Vietnam 18*, 235-241.
- [7] Duxson, P., & Provis, J. L. (2008). Designing precursors for geopolymer cements. *Journal of the American Ceramic Society*, 91(12), 3864–3869. doi:10.1111/j.1551-2916.2008.02787.x.
- [8] De Silva, P., Sagoe-Crenstil, K., & Sirivivatnanon, V. (2007). Kinetics of geopolymerization: Role of Al₂O₃ and SiO₂. *Cement and Concrete Research*, 37(4), 512–518. doi:10.1016/j.cemconres.2007.01.003.
- [9] Duxson, P., Mallicoat, S. W., Lukey, G. C., Kriven, W. M., & van Deventer, J. S. J. (2007). The effect of alkali and Si/Al ratio on the development of mechanical properties of metakaolin-based geopolymers. *Colloids and Surfaces A: Physicochemical and Engineering Aspects*, 292(1), 8–20. doi:10.1016/j.colsurfa.2006.05.044.
- [10] Fletcher, R. A., MacKenzie, K. J. D., Nicholson, C. L., & Shimada, S. (2005). The composition range of aluminosilicate geopolymers. *Journal of the European Ceramic Society*, 25(9), 1471–1477. doi:10.1016/j.jeurceramsoc.2004.06.001.
- [11] Autef, A., Joussein, E., Gasgnier, G., & Rossignol, S. (2012). Role of the silica source on the geopolymerization rate. *Journal of Non-Crystalline Solids*, 358(21), 2886–2893. doi:10.1016/j.jnoncrysol.2012.07.015.
- [12] Diaz, E. I., Allouche, E. N., & Eklund, S. (2010). Factors affecting the suitability of fly ash as source material for geopolymers. *Fuel*, 89(5), 992–996. doi:10.1016/j.fuel.2009.09.012.
- [13] Williams, R. P., & Van Riessen, A. (2010). Determination of the reactive component of fly ashes for geopolymer production using XRF and XRD. *Fuel*, 89(12), 3683–3692. doi:10.1016/j.fuel.2010.07.031.
- [14] van Jaarsveld, J. G. S., Van Deventer, J. S. J., & Lukey, G. C. (2003). The characterisation of source materials in fly ash-based geopolymers. *Materials Letters*, 57(7), 1272–1280. doi:10.1016/S0167-577X(02)00971-0.
- [15] Brouwers, H. J. H., & Van Eijk, R. J. (2002). Fly ash reactivity: Extension and application of a shrinking core model and thermodynamic approach. *Journal of Materials Science*, 37(10), 2129–2141. doi:10.1023/A:1015206305942.
- [16] Pietersen, H. S., Fraay, A. L. A., & Bijen, J. M. (1989). Reactivity of Fly Ash At High pH. *MRS Proceedings*, 178, 139–157. doi:10.1557/proc-178-139.
- [17] Chen-Tan, N. W., Van Riessen, A., Ly, C. V., & Southam, D. C. (2009). Determining the reactivity of a fly ash for production of geopolymer. *Journal of the American Ceramic Society*, 92(4), 881–887. doi:10.1111/j.1551-2916.2009.02948.x.
- [18] Fernández-Jiménez, A., Palomo, A., Sobrados, I., & Sanz, J. (2006). The role played by the reactive alumina content in the alkaline activation of fly ashes. *Microporous and Mesoporous Materials*, 91(1–3), 111–119. doi:10.1016/j.micromeso.2005.11.015.
- [19] Al-Shathr, B. S., Al-Attar, T. S., & Hasan, Z. A. (2016). Effect of curing system on metakaolin based geopolymer concrete. *Journal of University of Babylon*, 24(3), 569-576.
- [20] Shamsa, M. H., Al-Shathr, B. S., & Al-Attar, T. S. (2018). Effect of Pozzolan Materials on Compressive Strength of Geopolymer Concrete. *Kufa Journal of Engineering*, 9(3), 26–36. doi:10.30572/2018/kje/090303.
- [21] Dvorkin, L., Bordiuzhenko, O., Zhitkovsky, V., & Marchuk, V. (2019). Mathematical modeling of steel fiber reinforced concrete properties and selecting its effective composition. *IOP Conference Series: Materials Science and Engineering*, 708(1), 012085. doi:10.1088/1757-899x/708/1/012085.
- [22] Iraqi Specification No. 45. (1984). *Natural Aggregate Resource That Used in Building and Concrete (Vol. 45)*. Iraqi Specification Standard, Baghdad, Iraq. (In Arabic).
- [23] ASTM C494/C494M – 17. (2017). *Standard Specification for Chemical Admixtures for Concrete*. ASTM International, Pennsylvania, United States.
- [24] Al-Shathr, B. S., Al-Attar, T. S., & Hasan, Z. A. (2016). Effect of curing system on metakaolin based geopolymer concrete. *Journal of University of Babylon*, 24(3), 569-576.
- [25] Bernal, S. A., Mejía De Gutiérrez, R., & Provis, J. L. (2012). Engineering and durability properties of concretes based on alkali-activated granulated blast furnace slag/metakaolin blends. *Construction and Building Materials*, 33, 99–108. doi:10.1016/j.conbuildmat.2012.01.017.
- [26] Alhifadhi, M. A. (2015). *Structural Behavior of Reinforced Fly Ash Based Geopolymer Concrete T-beams*. PhD thesis, University of Technology, Baghdad, Iraq.

- [27] Bernal, S. A., Mejía De Gutiérrez, R., & Provis, J. L. (2012). Engineering and durability properties of concretes based on alkali-activated granulated blast furnace slag/metakaolin blends. *Construction and Building Materials*, 33, 99–108. doi:10.1016/j.conbuildmat.2012.01.017.
- [28] Giannopoulou, I., Dimas, D., Maragkos, I., & Pantias, D. (2009). Utilization of metallurgical solid by-products for the development of inorganic polymeric construction materials. *Global Nest Journal*, 11(2), 127–136. doi:10.30955/gnj.000589.
- [29] Mijarsh, M. J. A., Megat Johari, M. A., & Ahmad, Z. A. (2015). Effect of delay time and Na₂SiO₃ concentrations on compressive strength development of geopolymer mortar synthesized from TPOFA. *Construction and Building Materials*, 86, 64–74. doi:10.1016/j.conbuildmat.2015.03.078.
- [30] Weng, L., & Sagoe-Crentsil, K. (2007). Dissolution processes, hydrolysis and condensation reactions during geopolymer synthesis: Part I-Low Si/Al ratio systems. *Journal of Materials Science*, 42(9), 2997–3006. doi:10.1007/s10853-006-0820-2.
- [31] Duxson, P., Provis, J. L., Lukey, G. C., Mallicoat, S. W., Kriven, W. M., & van Deventer, J. S. J. (2005). Understanding the relationship between geopolymer composition, microstructure and mechanical properties. *Colloids and Surfaces A: Physicochemical and Engineering Aspects*, 269(1-3), 47–58. doi:10.1016/j.colsurfa.2005.06.060.
- [32] Kupwade-Patil, K., & Allouche, E. N. (2013). Impact of Alkali Silica Reaction on Fly Ash-Based Geopolymer Concrete. *Journal of Materials in Civil Engineering*, 25(1), 131–139. doi:10.1061/(asce)mt.1943-5533.0000579.
- [33] Kusbiantoro, A., Nuruddin, M. F., Shafiq, N., & Qazi, S. A. (2012). The effect of microwave incinerated rice husk ash on the compressive and bond strength of fly ash based geopolymer concrete. *Construction and Building Materials*, 36, 695–703. doi:10.1016/j.conbuildmat.2012.06.064.
- [34] Partha, S. D., Pradip, N., & Prabir, K. S. (2013). Strength and permeation properties of slag blended fly ash based geopolymer concrete. *Advanced Materials Research*, 651, 168–173. doi:10.4028/www.scientific.net/AMR.651.168.
- [35] Nuruddin, M. F., Demie, S., & Shafiq, N. (2011). Effect of mix composition on workability and compressive strength of self-compacting geopolymer concrete. *Canadian Journal of Civil Engineering*, 38(11), 1196–1203. doi:10.1139/111-077.
- [36] Joseph, B., & Mathew, G. (2012). Influence of aggregate content on the behavior of fly ash based geopolymer concrete. *Scientia Iranica*, 19(5), 1188–1194. doi:10.1016/j.scient.2012.07.006.
- [37] Noushini, A., & Castel, A. (2016). The effect of heat-curing on transport properties of low-calcium fly ash-based geopolymer concrete. *Construction and Building Materials*, 112, 464–477. doi:10.1016/j.conbuildmat.2016.02.210.
- [38] Samdani, G. & Quadar, G. (2017). A study of geopolymer concrete as sustainable cementless concrete. *Global Journal of Engineering Science and Researches*, 4(9), doi:10.5281/zenodo.999313.
- [39] Divvala, S., & Rani, M. S. (2021). Strength properties and durability studies on modified geopolymer concrete composites incorporating GGBS and metakaolin. *Applied Nanoscience*. doi:10.1007/s13204-021-02015-y.
- [40] Mallikarjuna Rao, G., & Gunneswara Rao, T. D. (2018). A quantitative method of approach in designing the mix proportions of fly ash and GGBS-based geopolymer concrete. *Australian Journal of Civil Engineering*, 16(1), 53–63. doi:10.1080/14488353.2018.1450716.
- [41] Arun, B. R., Nagaraja, P. S., & Srishaila, J. M. (2018). An Effect of NaOH Molarity on Fly Ash—Metakaolin-Based Self-Compacting Geopolymer Concrete. *Sustainable Construction and Building Materials*, 233–244. doi:10.1007/978-981-13-3317-0_21.
- [42] Nguyen, K. T., Lee, Y. H., Lee, J., & Ahn, N. (2013). Acid Resistance and Curing Properties for Green Fly Ash-geopolymer Concrete. *Journal of Asian Architecture and Building Engineering*, 12(2), 317–322. doi:10.3130/jaabe.12.317.
- [43] Ryu, G. S., Ahn, G. H., Koh, K. T., & Lee, J. H. (2013). Compressive strength properties of fly ash-based geopolymer concrete. *Advanced Materials Research*, 741, 49–54. doi:10.4028/www.scientific.net/AMR.741.49.
- [44] Albitar, M., Mohamed Ali, M. S., Visintin, P., & Drechsler, M. (2015). Effect of granulated lead smelter slag on strength of fly ash-based geopolymer concrete. *Construction and Building Materials*, 83, 128–135. doi:10.1016/j.conbuildmat.2015.03.009.
- [45] Sellar, T., & Arulrajah, A. A. (2018). The Role of Social Support on Job Burnout in the Apparel Firm. *International Business Research*, 12(1), 110-118. doi:10.5539/ibr.v12n1p110.
- [46] De Larrard, F., & Malier, Y. (1992). Engineering properties of very high performance concrete. *High Performance Concrete, from Material to Structure*, 85-114.
- [47] Favre, R., & Charif, H. (1994). Basic model and simplified calculations of deformations according to the CEB-FIP model code 1990. *ACI Structural Journal*, 91(2), 169–177. doi:10.14359/4602.
- [48] Gardner, N. J., & Poon, S. M. (1976). Time and Temperature Effects on Tensile, Bond, and Compressive Strengths. *J Am Concr Inst*, 73(7), 405–409. doi:10.14359/11081.

- [49] Ramujee, K., & Potharaju, M. (2017). Mechanical Properties of Geopolymer Concrete Composites. *Materials Today: Proceedings*, 4(2), 2937–2945. doi:10.1016/j.matpr.2017.02.175.
- [50] Raphael, J. M. (1984). Tensile Strength of Concrete. *Journal of the American Concrete Institute*, 81(2), 158–165. doi:10.1007/978-3-642-41714-6_200519.
- [51] Ryu, G. S., Lee, Y. B., Koh, K. T., & Chung, Y. S. (2013). The mechanical properties of fly ash-based geopolymer concrete with alkaline activators. *Construction and Building Materials*, 47, 409–418. doi:10.1016/j.conbuildmat.2013.05.069.
- [52] Zaetang, Y., Wongsas, A., Sata, V., & Chindapasirt, P. (2015). Use of coal ash as geopolymer binder and coarse aggregate in pervious concrete. *Construction and Building Materials*, 96, 289–295. doi:10.1016/j.conbuildmat.2015.08.076.
- [53] ACI 318R-14. (2014). *Building Code Requirements for Structural Concrete and Commentary*. Building Code Requirements for Structural Concrete and Commentary, American concrete institute, Michigan, United States.
- [54] Albitar, M., Visintin, P., Mohamed Ali, M. S., & Drechsler, M. (2015). Assessing behaviour of fresh and hardened geopolymer concrete mixed with class-F fly ash. *KSCE Journal of Civil Engineering*, 19(5), 1445–1455. doi:10.1007/s12205-014-1254-z.
- [55] Hardjito, D., & Rangan, B. (2005). *Development and Properties of Low Calcium Fly Ash*. Curtin University of Technology, Perth, Australia. Available online: https://espace.curtin.edu.au/bitstream/handle/20.500.11937/5594/19327_downloaded_stream_419.pdf?sequence=2&isAllowed=y (accessed on December 2021).
- [56] Raijiwala, D. B., & Patil, H. S. (2010). Geopolymer concrete A green concrete. 2nd International Conference on Chemical, Biological and Environmental Engineering, (2-4 Nov. 2010), Cairo, Egypt. doi:10.1109/icbee.2010.5649609
- [57] Nguyen, N. H., Smith, S. M., Staniford, M. D., & van Senden, M. F. (2010). Geopolymer concrete—Concrete goes green. Research report, School of Civil, Environmental and Mining Engineering, The University of Adelaide, Adelaide, Australia.
- [58] Olivia, M., & Nikraz, H. (2012). Properties of fly ash geopolymer concrete designed by Taguchi method. *Materials and Design*, 36, 191–198. doi:10.1016/j.matdes.2011.10.036.
- [59] Fernández-Jiménez, A. M., Palomo, A., & López-Hombrados, C. (2006). Engineering properties of alkali-activated fly ash concrete. *ACI Materials Journal*, 103(2), 106–112. doi:10.14359/15261.